# Study of the Mechanical Properties of Some Structural Aluminium-Steel Joints

**Leonardo Rodrigues Danninger**
Instituto de Pesquisas Tecnológicas do Estado de São Paulo
Escola Politécnica da USP

**Ana Paola Villalva Braga**
Instituto de Pesquisas Tecnológicas do Estado de São Paulo

**Marcelo Gonçalves**
Alpina Consultoria Tecnológica e Educacional

**ABSTRACT**

In a world in which vehicles of higher energy efficiency have constantly been pursued, the development of multi-material structures can be extremely interesting as far as structural weight reduction and the mitigation of greenhouse gas emissions are concerned. This paper evaluates basic mechanical properties of vehicular structural joints between commercial grades aluminium alloys and grade steels. These joints were produced by either riveting or adhesive bonding techniques, currently used as standard procedures in the automotive industry. Five types of joints were studied: three were adhesively bonded and two were riveted. For each joint, basic mechanical properties were measured via tensile and fatigue tests.

The tensile tests of the riveted joints have shown that the failure has constantly occurred associated to the fracture at the rivets, whereas for the adhesively bonded joints a cohesive fracture has always occurred regardless of the characteristics of the joint. The data from the fatigue tests could be well fitted to Wöhler S-N curves, so that fatigue limits for all joints could be obtained. Thus, this technology research has shown the feasibility of using adhesive bonding and riveting techniques to successfully join multi-material structures to be used in the automotive industry.

## 1. INTRODUCTION

Joining is an important process in manufacturing of most products in modern times and the selection of an appropriate joining technique is a key factor to enable innovative and sustainable manufacturing [1]. Over the years, the automotive industry have sought to reduce the mass of their structures, seeking greater energy efficiency and mitigation of greenhouse gas (GHG) emissions, while maintaining the safety of their vehicles [2].

The pursuit of lighter, stronger, and more efficient structures has led to the development of innovative solutions for joining different materials, such as metals, polymers, ceramics, and composites. However, the differences in physical and chemical properties of these materials, as well as the occurrence of adverse effects during the joining process presents significant challenges. According to Peroni et al. [3] one of the great difficulties in developing multi-material structures by joining dissimilar metals is to ensure structural integrity after joining, which is critical to maintaining the crashworthiness of well-designed structure.

The joining of multi-materials structures usually requires the use of different joining techniques, such as adhesive and mechanical fasteners [4], each with its advantages and disadvantages. Mechanical fasteners are widely used to joint dissimilar materials and are, from a technological point of view, a more consolidated and known solution, however there exist some apparent disadvantages such as high stress concentration and destruction of structural integrity [5]. On the other hand, adhesive bonding features a more uniform stress distribution along the joint, in addition to corrosion resistance, although issues such as curing time and lack of knowledge about the factors that affect the performance of this type of joint limit its application [2, 5]. As acknowledged by Kanani, A. Y. et al. [2], when considering the production of multi-material joints in automotive structures, the financial feasibility of the assembling procedure is just as critical as the required mechanical strength of joints.

This study is part of the research project developed by the Institute for Technological Research (IPT) entitled: "*Desenvolvimento de Sistema para Comparação do Desempenho de juntas de Ligas de Alumínio em Estruturas de Veículos Automotores (Development of a System for Comparing the Performance of Aluminum Alloy Joints in Automotive Vehicle Structures)"*. While the research project focused on the comparative analysis of different joints, the current study focuses only on the mechanical response of dissimilar multi-materials riveted and adhesive joints to lap shear-loading conditions. Five joints made of dissimilar materials that can be applied in automotive structures were selected for this study. For each joint studied, the specimens were prepared and test under tensile shear test and fatigue test. The mechanical properties were evaluated in order to demonstrate the possibility of using adhesive bonding and riveting techniques to successfully join multi-material structures to be used in the automotive industry.

## 2. EXPERIMENTAL

### *2.1 SPECIMENS PREPARATION*

In this study, seven different materials were involved for preparing the adhesive and riveted joints: three steel grades (IF 180 GI, LNE 500 and LNE 26 steel) and four commercial aluminium grades (AA5182-O, AA6005A-T6, AA6082-T6 and AA7046-T6). The materials and joint method are listed in Table 1.

**Table 1**. Identification and characteristics of joints

| Identification | Process | Aluminium (thickness) | Steel (thickness) |
|---|---|---|---|
| **J1** | **Adhesive** | 5182-O (2.5 mm) | IF 180 GI (0.9 mm) |
| **J2** | **Adhesive** | 6005A-T6 (2.0 mm) | LNE 26 (6.0 mm) |
| **J3** | **Adhesive** | 6082-T6 (5.0 mm) | LNE 500 (5.0 mm) |
| **J4** | **Riveted** | 7046-T6 (2.0 mm) | LNE 500 (2.0 mm) |
| **J5** | **Riveted** | 6082-T6 (5.0 mm) | LNE 500 (5.0 mm) |

For the adhesive joints, from the materials listed above, substrates of 114.3 mm in length and 25.4 mm in width were made. After this step, the substrates were cleaned with methyl-ethyl ketone (MEK) and the acrylic-based adhesive LORD® 852/25GB was prepared by mixing the adhesive with the catalyst LORD® Accelerator 25GB to perform the bonding, which was performed following the ASTM D1002 standard. At least 22 specimens were produced with the geometry shown in figure 1 for each type of adhesive joint.

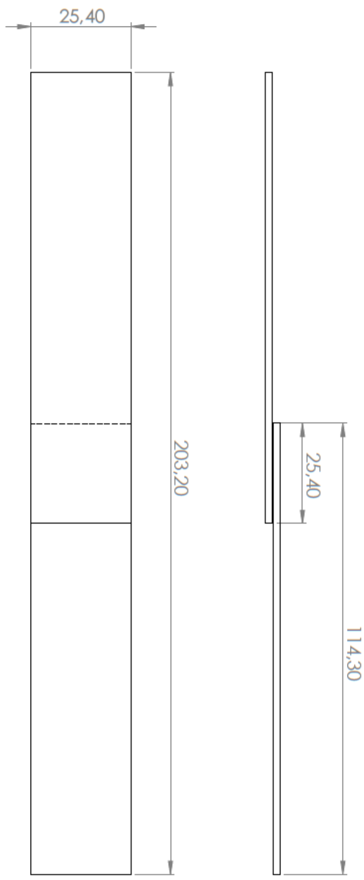


**Figure 1.** Geometry of the adhesive specimens. The thickness of the plates varies according to the joint (image not to scale).

For the riveted joints, from the materials listed above, substrates of 147.5 mm in length, 45.0 mm in width with a 6.5 mm diameter hole in one of the ends for positioning the rivet were made. After this step, the previously made holes were aligned and the rivet was applied. The specimens geometry were based on standardized tests that Bollhoff already performs to evaluate the performance of its products intended for the automotive market. The Rivquick® Varilock mechanical fastener was selected for this study because of its fatigue performance according to the manufacturer and market availability; and for its application the Bollhoff P3000 assembly tool was used. At least 22 specimens were produced with the geometry shown in figure 2 for each type of riveted joint.

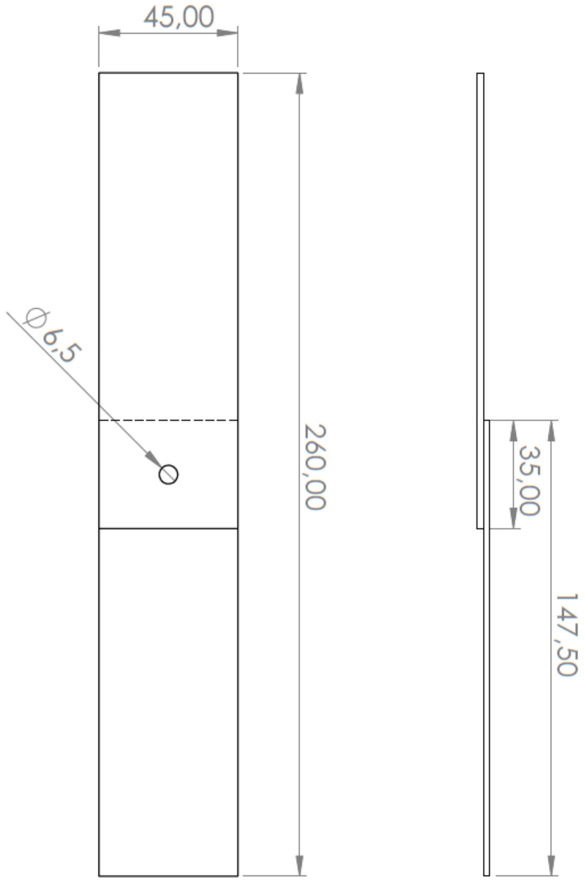


**Figure 2.** Geometry of the riveted specimens. The thickness of the plates varies according to the joint (image not to scale).

*2.2 TENSILE TEST*

The tensile tests of the adhesive and riveted joints were conducted under quasi-static condition in a 100 kN testing machine (MTS 100 kN materials testing system) with displacement control mode at a speed of 1.5 mm/min. All the specimens were test in the same testing machine and without the use of shims.

At least three CPs of each joint were tested, after the tests, the CPs were identified, and the fractures characterized with the aid of macrographs for later attempts to correlate them with the observed mechanical behavior. With the data recorded by the equipment, the maximum forces for each joint were determined.

*2.3 FATIGUE TEST*

Fatigue tests were conducted in the same equipment used for the tensile test (MTS 100 kN materials testing system), in force control mode and with a stress ratio (R) of 0 and a frequency of 15 Hz. The strength levels used in the tests were defined as fractions of the maximum force obtained in the static tests. The selected fractions were 67%, 50%, 30% and 20%. Such fractions were selected based on the MIL-STD-1312-21 standard.

The tests were carried out until the sample fractured or the sample reached a run-out of 1.00E+7 cycles. Each strength level of each joint was tested in replica (two samples for each fraction of maximum force). After the tests, the date were fitted to Wöhler S-N curves, so that fatigue limits (maximum force for the joint achieve 1.00E+7 cycles) for all joints could be obtained.

## 3. RESULTS AND DISCUSSION

*3.1 ADHESIVE JOINTS*

The maximum force of the adhesive joints are present in Table 2 and Figure 3.

**Table 2**. Measured failure force for the adhesive joints

| Joint | Maximum Force (N) | | | |
|---|---|---|---|---|
| | **Test 1** | **Test 2** | **Test 3** | **Average** |
| **J1** | 8318.72 | 8160.57 | 7633.96 | **8037.75** |
| **J2** | 11195.42 | 11157.79 | 10011.69 | **10788.30** |
| **J3** | 11263.17 | 9567.59 | 10298.95 | **10376.57** |

As expected, the failure in all samples tested in the tensile test is due a cohesive failure, indicating that there were no adhesion problems between the adhesive and the aluminum substrates or steel substrates. Figure 4 shows, as an example, the cohesive fracture observed for joint J2

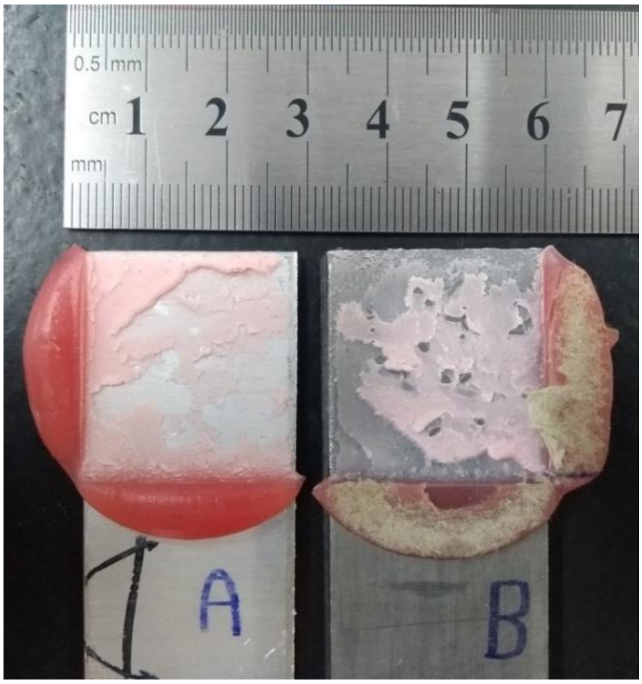


**Figure 4.** Detail of cohesive fracture in sample J2 **-** test 1

Despite the fact that the same adhesive was used (LORD® 852/25GB), as well as the overlapping area being the same (645 mm²) and the same bonding methodology being used for all adhesive joints, it is possible to verify that there is a differences in the maximum strength of each bonded joint. This observation can be related to the way in which loading occurs in this type of joint [4]: a moment is generated at the bond interface when this geometry of sample is loaded due the offset of the adherends/substrates corresponding to the thickness of the adhesive and half thicknesses of the adherends, leading to the bending of the adherends and the induction of a normal (Mode I) loading. The emergence of this mode of loading, associated with the intended primary mode of loading in this type of testing (Mode II – shear), results in a mixed-mode stress state at the ends of the bond line [6]

Therefore, it is possible to consider that the differences between the observed maximum forces are directly related to the geometry of the joint and the appearance of this moment that alters the stress state of the joint. According to Watson, B et al [4], this bending can be reduced, if desired, by using thicker adherends (substrates); however, this may result in a characterization of the adhesive and not the intended joint.

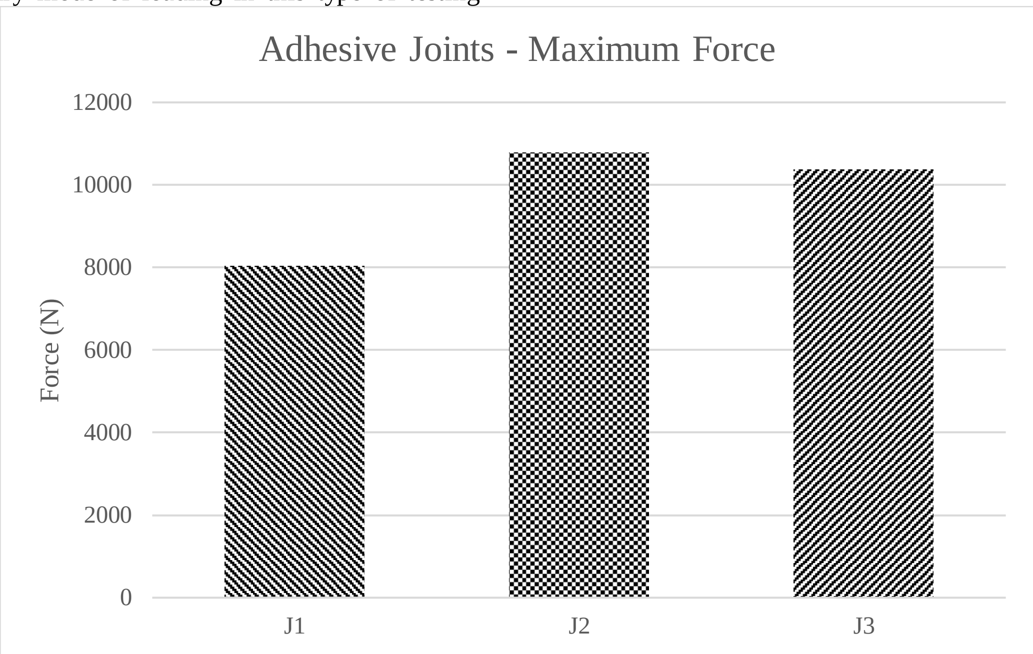


**Figure 3.** Average maximum force at failure for each adhesive joint

Another factor that can affect the mechanical behavior of bonded joints is related to the mechanical properties of the substrates, in particular, the Young's modulus. According to Kanani et al. [2] shear stress concentrations are higher near the free edge of the interface between the adhesive and lower Young's modulus adherend/substrate resulting in asymmetric stress distribution due to different longitudinal deformations at the overlap edges.

Figure 5 shows the linear fit from the Wöhler S-N curves for each adhesive joint. An analysis of the regressions reveals that they all have a coefficient ($R^2$) greater than 0.8, indicating a good linear fit, so that the respective first degree equations can be used to determine the fatigue limit. Such equations, as well as the respective fatigue limits calculated for each joint are presented in table 3.

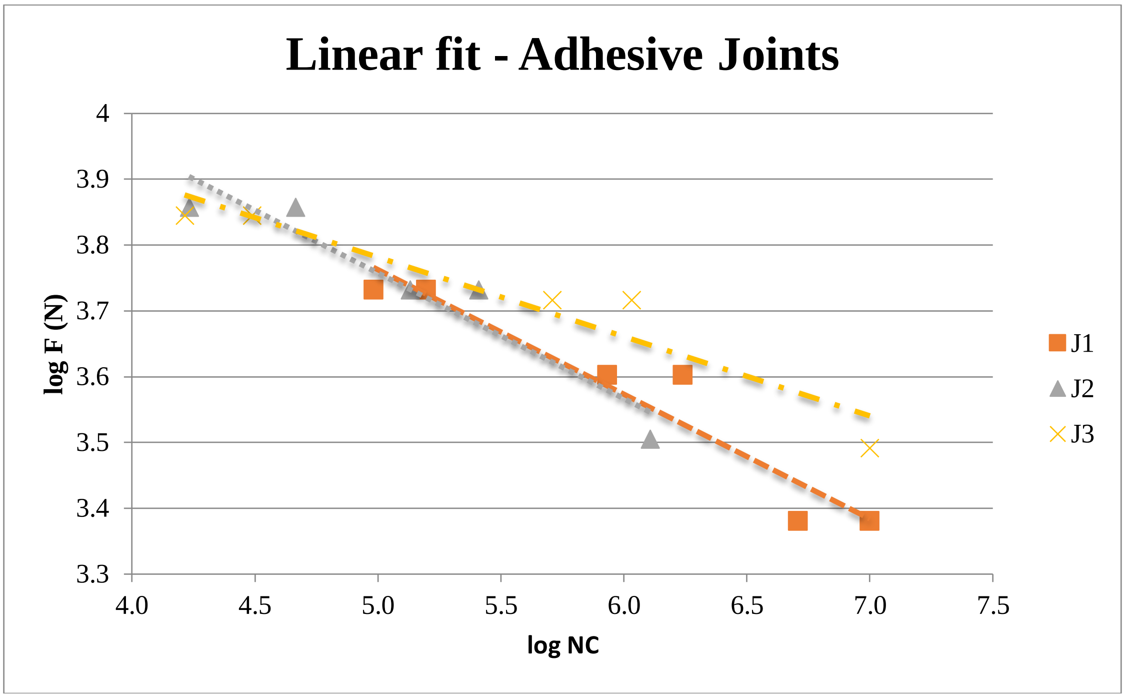


**Figure 5.** Linear Fit for the adhesive joints

**Table 3**. Fatigue limit for adhesive joints

| Joint | First Degree equation (y = ax+b) | | Fatigue limit (N) |
|---|---|---|---|
| | a | b | |
| J1 | -0.1893 | 4.7094 | 2423 |
| J2 | -0.1909 | 4.7120 | 2375 |
| J3 | -0.1206 | 4.3844 | 3469 |

In the dataset, two types of failure occurred: metallic substrate failure and cohesive failure; substrate failures were predominant in joints with thinner substrates (joints J1 and J2), while cohesive failures were predominant in joint J3 with thicker substrates. For a plane stress state, Pereira et al [7] found that an increase in substrate thickness leads to an increase in the stress peak in the adhesive region, which may help explain why failure occurs predominantly cohesively in the J3.

*3.2 RIVETED JOINTS*

The maximum force of the riveted joints are present in Figure 6 and Table 4.

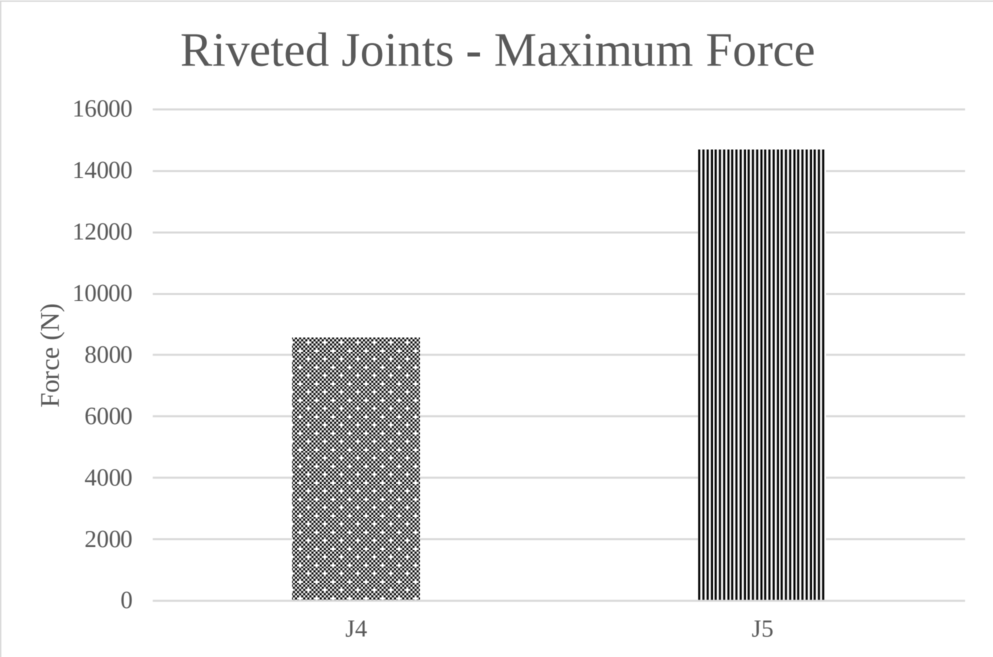


**Figure 6.** Average maximum force at failure for each riveted joint

**Table 4**. Measured failure force for the riveted joints

| Joint | Maximum Force (N) | | | |
|---|---|---|---|---|
| | **Test 1** | **Test 2** | **Test 3** | **Average** |
| **J4** | 8452.52 | 8586.77 | 8638.97 | 8559.42 |
| **J5** | 14246.92 | 15122.42 | 14669.87 | 14679.74 |

For both riveted joints, it was observed that joint failure occurred through fracture of the rivet body, as well as the occurrence of a deformation of the hole in the aluminum substrate. Figure 7 is presented as an example of the failures observed in the tensile tests of riveted joints.

As with adhesive joints, due to the geometry of the samples, the joints are subject to a mixed-mode stress state that will affect the mechanical performance of the joint. According to Mucha e Witkowski [8], the stress concentrations appear on the contact surface of the body of the rivet and the hole and the hole surface is deformed until the maximum rivet load capacity in the transverse cross-section is reached, after that the rivet material fracture.

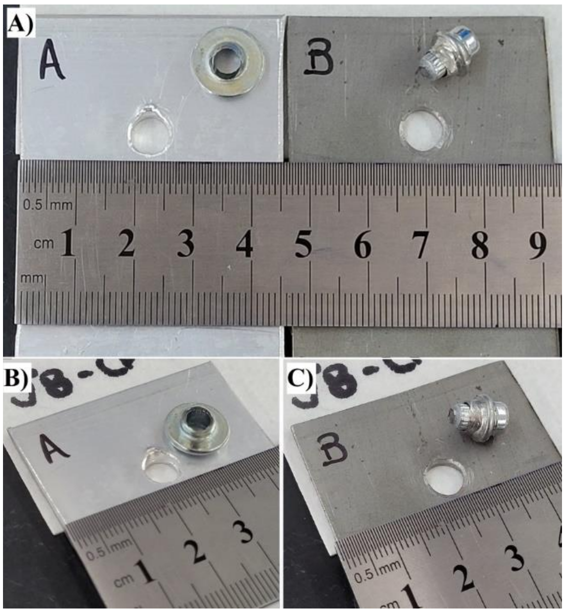


**Figure 7.** Fracture of sample J4 - test 1. A) Macrograph; B)AA7046-T6 substrate C) LNE 500 substrate.

Figure 8 shows the linear fit from the Wöhler S-N curves for each riveted joint. A similar analysis of the regressions to that made for the adhesive joints, reveals a coefficient ($R^2$) greater than 0,9, so that indicates a good linear fit and the first degree equations can be used to determine the fatigue limit. Such equations, as well as the respective fatigue limits calculated for each joint are presented in table 5.

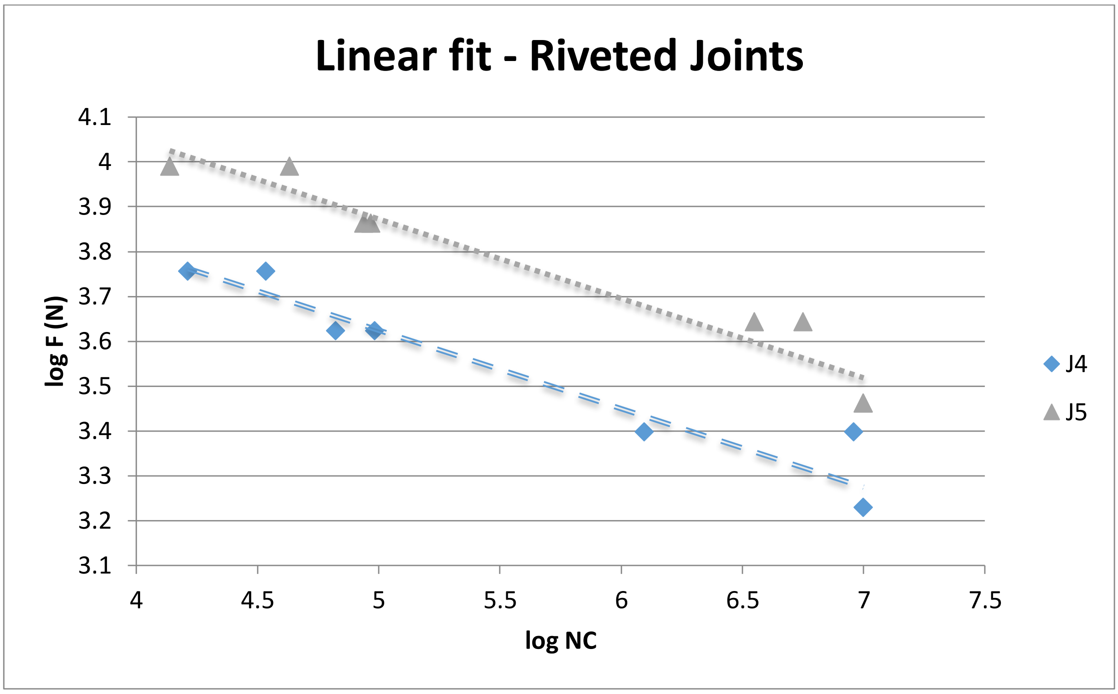


**Figure 8.** Linear Fit for the riveted joints

**Table 5**. Fatigue limit for riveted joints

| Joint | First Degree equation (y = ax+b) | | Fatigue limit (N) |
|---|---|---|---|
| | a | b | |
| J4 | -0.1750 | 4.4995 | 1881 |
| J5 | -0.1771 | 4.7578 | 2375 |

An analysis of the fatigue results reveals that two failure modes can occur during fatigue tests: rivet failure, occurring through rupture of the rivet body, and plate failure, which occurs due to fracture of the substrate in the region of the hole. According to Skorupa et al. [9], even in the simplest cases of riveted joints tested under uniaxial loading, as is the case of the samples tested in this study, the fatigue behavior can be affected by four main variables: the type of rivet, application, substrate thickness and applied load. The fatigue behavior of a riveted joint is influenced by several factors, which explains the variation in the failure mode; however, for a more detailed understanding of this behavior, it is necessary to carry out a more in-depth study.

## 4. CONCLUSIONS

The study and development of dissimilar multi-material joints represent a promising area for engineering, offering significant potential to drive innovation and technological progress in several industrial sectors, including the automotive industry. The combination of different materials makes it possible to develop and manufacture optimized vehicle structures aimed at reducing weight.

This technology research has shown the feasibility of using adhesive bonding and riveting techniques to successfully join dissimilar multi-material structures to be used in the automotive industry. However, it is important to highlight that there are still challenges to overcome and a greater understanding of both the joining techniques and the interactions between the different materials is necessary to expand and disseminate the use of this type of joint.

## ACKNOWLEDGMENTS

The authors would like to thank the Brazilian Company for Industrial Research and Innovation (EMBRAPII), the Brazilian Aluminum Association (ABAL) and all the partner companies in the JUNTAS Project – Aethra, Böllhoff, CBA, ESAB, FSW Brasil, Hydro Extrusion, Maxion Structures, Metalsa, Novelis, Parker LORD, Prolind, Randon, Stellantis, ReciclaBR and Transvalor Brasil – for their collaboration in carrying out this work

## REFERENCES

[1] DIAS, G. K.; SAKUNDARINI, N.; MAY MAY, C. C. Mechanical and Failure Analysis of Multi-Materials Adhesive Joining. **International Journal of Integrated Engineering**, *[S. l.]*, v. 13, n. 7, p. 160–166, 2021 Artigo Dias, G. K. Mechanical and Failure.

[2] KANANI, A. Y. *et al*. Hybrid and adhesively bonded joints with dissimilar adherends: a critical review. **Journal Of Adhesion Science And Technology**, [S.L.], v. 35, n.

17, p. 1821-1859, 22 dez. 2020. Informa UK Limited.Artigo Yousefi Kanani

[3] PERONI, L.; AVALLE, M.; BELINGARDI, G. Comparison of the energy absorption capability of crash boxes assembled by spot-weld and continuous joining techniques. **International Journal Of Impact Engineering**, [S.L.], v. 36, n. 3, p. 498-511, mar. 2009. Elsevier BV.

[4] WATSON, B. *et al*. Metallic multi-material adhesive joint testing and modeling for vehicle lightweighting. **International Journal Of Adhesion And Adhesives**, [S.L.], v. 95, p. 102421, dez. 2019. Elsevier BV.Artigo Watson

[5] SUN, G. *et al*. On fracture characteristics of adhesive joints with dissimilar materials – An experimental study using digital image correlation (DIC) technique. **Composite Structures**, [S.L.], v. 201, p. 1056-1075, out. 2018. Elsevier BV.

[6] GONÇALVES, J.P.M; MOURA, M.F.s.F de; CASTRO, P.M.s.T de. A three-dimensional finite element model for stress analysis of adhesive joints. **International Journal Of Adhesion And Adhesives**, [S.L.], v. 22, n. 5, p. 357-365, jan. 2002. Elsevier BV.

[7] PEREIRA, A.M. *et al*. Study on the fatigue strength of AA 6082-T6 adhesive lap joints. **International Journal Of Adhesion And Adhesives**, [S.L.], v. 29, n. 6, p. 633-638, set. 2009. Elsevier BV.

[8] MUCHA, J.; WITKOWSKI, W. The Structure of the Strength of Riveted Joints Determined in the Lap Joint Tensile Shear Test. **Acta Mechanica Et Automatica**, [S.L.], v. 9, n. 1, p. 44-49, 1 mar. 2015. Walter de Gruyter GmbH.

[9] SKORUPA, A. *et al*. Fatigue crack location and fatigue life for riveted lap joints in aircraft fuselage. **International Journal Of Fatigue**, [S.L.], v. 58, p. 209-217, jan. 2014. Elsevier BV.